condensed matter

MDPI

Article

Features of Light-Matter Coupling in Non-Ideal Lattice of Coupled Microcavities Containing Quantum Dots

Vladimir V. Rumyantsev [1,2,*], Stanislav A. Fedorov [1], Konstantin V. Gumennyk [1] and Alexey Ye. Rybalka [1]

[1] A.A. Galkin Donetsk Institute for Physics and Engineering, 83114 Donetsk, Russia
[2] Mediterranean Institute of Fundamental Physics, Marino, 00047 Rome, Italy
* Correspondence: vladimir.rumyantsev2011@yandex.ru

Abstract: In this paper, within the framework of virtual crystal approximation, the mathematical modeling of the dependence of the density of states of polariton excitations in a 1D photonic crystal—a system of pores (tunnel-coupled microresonators) containing quantum dots—on the concentration of structural defects is performed.

Keywords: energy spectrum of polariton excitations; imperfect 1D photonic crystal; structural defects; virtual crystal approximation

Citation: Rumyantsev, V.V.; Fedorov, S.A.; Gumennyk, K.V.; Rybalka, A.Y. Features of Light-Matter Coupling in Non-Ideal Lattice of Coupled Microcavities Containing Quantum Dots. *Condens. Matter* **2023**, *8*, 41. https://doi.org/10.3390/condmat8020041

Academic Editors: Alexey Kavokin and Helgi Sigurdsson

Received: 20 February 2023
Revised: 26 April 2023
Accepted: 29 April 2023
Published: 2 May 2023

1. Introduction

Currently, the creation of cutting-edge nanocomposite-based sources of coherent radiation and the building of them into user-ready devices entails the necessity of an adequate conceptual understanding of nanocrystalline photonic systems [1,2]. One of the challenges encountered on this path deals with the study of the properties of the so-called polaritonic crystals [3]. The latter constitute a special class of photonic crystals [4] exhibiting a strong coupling between the quantum excitation of media (excitons) and optical fields. Hence, we have seen the emergence of polaritonics as a subdiscipline of photonics.

As examples of polaritonic structures, one can mention, e.g., the spatially periodic systems of coupled microcavities (microresonators) [5,6], along with the arrays of quantum dots (QDs) embedded in photonic nanostructures [7,8]. Lately, there has been an increasing interest in optical modes when used in the combined media of microresonators and quantum dots. Ref. [9] offers evidence for the realization of a strong coupling between a QD and a microresonator. It is worth mentioning various studies [3,8] devoted to the coupling of quantum solitons to lower-dispersion-branch (LDB) polaritons in a microresonator chain. It is conjectured therein that microresonators may serve as constituent elements for the creation of quantum information processing devices.

Another actively developing field is that of the photonics of imperfect structures. For instance, the authors of Refs. [9–11] examine the effect of structural defects on the dispersion of polaritonic excitations in a lattice of tunnel-coupled microresonators with embedded QDs and that of exciton-like excitations in microcavities with no QDs. Calculational methods in the photonics of imperfect structures permit researchers to demonstrate that the introduction of structural defects, along with various kinds of external actions (elastic deformation being one of them [12]), results in a substantial alteration of the energy spectrum of electromagnetic excitations and of the optical properties of an overall structure.

Investigations into the density of energy states hold a prominent place in the field of condensed matter physics. This has motivated the present study into the density of states of quasiparticle excitations in a defect-containing one-dimensional microcavity lattice with embedded quantum dots.

2. Theoretical Model

The general model of quasiparticle excitation in an ideal lattice of microcavities (resonators, which can be viewed as a photonic subsystem) with embedded nanoclusters (which can be viewed as an atomic subsystem) has previously been developed by us in Refs. [9–11,13]. Following this line of reasoning, in the theoretical model below, we assume that the density of the excited states of structural elements in photonic and atomic subsystems is small. This permits us to retain only the quadratic term $\hat{H}^{ex}$ (describing elementary excitations) in Hamiltonian, $\hat{H}$, which, within the one-level model and Heitler–London approximation [8,14], in the case of an ideal crystal takes the form:

$$\hat{H}^{ex} = \sum_{\substack{\mathbf{n},\mathbf{m},\alpha,\beta,\\ \lambda,\sigma}} D^{\lambda\sigma}_{\mathbf{n}\alpha,\mathbf{m}\beta}\hat{\Phi}^{+}_{\mathbf{n}\alpha\lambda}\hat{\Phi}_{\mathbf{m}\beta\sigma} = \sum_{\alpha,\beta=1}^{r}\sum_{\lambda,\sigma,\mathbf{k}} D^{\lambda\sigma}_{\alpha\beta}(\mathbf{k})\hat{\Phi}^{+}_{\alpha\lambda}(\mathbf{k})\hat{\Phi}_{\beta\sigma}(\mathbf{k}), \tag{1}$$

where $D^{\lambda\sigma}_{\alpha\beta}(\mathbf{k})$ is the Fourier transform of the matrix $D^{\lambda\sigma}_{\mathbf{n}\alpha\mathbf{m}\beta}$ (indices λ, σ assume values $1, 2$), and r is the number of structural elements in the crystal elementary cell.

$$\begin{aligned} &D^{11}_{\mathbf{n}\alpha,\mathbf{m}\beta} = \hbar\omega^{at}_{\mathbf{n}\alpha}\delta_{\mathbf{n}\alpha,\mathbf{m}\beta} + V_{\mathbf{n}\alpha,\mathbf{m}\beta},\ D^{22}_{\mathbf{n}\alpha,\mathbf{m}\beta} = \hbar\omega^{ph}_{\mathbf{n}\alpha}\delta_{\mathbf{n}\alpha,\mathbf{m}\beta} - A_{\mathbf{n}\alpha,\mathbf{m}\beta},\\ &D^{12}_{\mathbf{n}\alpha,\mathbf{m}\beta} = D^{21}_{\mathbf{n}\alpha,\mathbf{m}\beta} = g_{\vec{n}\alpha}\delta_{\mathbf{n}\alpha,\mathbf{m}\beta},\ \hat{\Phi}^{\lambda=2}_{\mathbf{n}\alpha} = \hat{\Psi}_{\mathbf{n}\alpha},\ \hat{\Phi}^{\lambda=1}_{\mathbf{n}\alpha} = \hat{B}_{\mathbf{n}\alpha} \end{aligned} \tag{2}$$

In expressions (1) and (2), $\omega^{ph}_{\mathbf{n}\alpha}$ is the photonic mode frequency of electromagnetic excitation localized at the $\mathbf{n}\alpha$-th node (resonator), $\hat{\Psi}^{+}_{\mathbf{n}\alpha}$, $\hat{\Psi}_{\mathbf{n}\alpha}$ are the Bose–Einstein creation and annihilation operators of this photonic mode in the node representation, $\hbar\omega^{at}_{\mathbf{n}\alpha}$ is the QD excitation energy at the $\mathbf{n}\alpha$-th node, $\hat{B}_{\mathbf{n}\alpha}$, $\hat{B}^{+}_{\mathbf{n}\alpha}$ are the Bose creation and annihilation operators of this excitation, $A_{\mathbf{n}\alpha\mathbf{m}\beta}$ is the matrix of resonance interaction, describing an overlap between the optical fields of resonators at the $\mathbf{n}\alpha$-th and $\mathbf{m}\beta$-th lattice sites and, thus, defining the tunneling probability of the corresponding electromagnetic excitation, $V_{\mathbf{n}\alpha\mathbf{m}\beta}$ is the resonance interaction matrix of QDs at the $\mathbf{n}\alpha$-th and $\mathbf{m}\beta$-th lattice sites, and $g_{\mathbf{n}\alpha}$ is the matrix of resonance interaction between QD at the $\mathbf{n}\alpha$-th site and the electromagnetic field localized at the same site. The indices λ, σ indicate the presence (value 1) or absence (value 2) of a QD at a corresponding cavity.

In equality (1), quantities $D^{\lambda\sigma}_{\alpha\beta}(\mathbf{k})$ and $\Phi_{\alpha\lambda}(\mathbf{k})$ take the form of $D^{\lambda\sigma}_{\alpha\beta}(\mathbf{k}) = \sum_{\mathbf{m}} D^{\lambda\sigma}_{\mathbf{n}\alpha\mathbf{m}\beta}\exp\left[i\mathbf{k}\cdot\left(\mathbf{r}_{\mathbf{n}\alpha} - \mathbf{r}_{\mathbf{m}\beta}\right)\right]$ and $\hat{\Phi}_{\alpha\lambda}(\mathbf{k}) = \frac{1}{\sqrt{N}}\sum_{\vec{n}}\hat{\Phi}_{\mathbf{n}\alpha\lambda}\exp(-i\mathbf{k}\cdot\mathbf{r}_{\mathbf{n}\alpha})$, where N is the number of elementary cells in the considered lattice. The wave vector $\mathbf{k}$, characterizing the eigenstates of electromagnetic excitations in the crystal, varies within the first Brillouin zone.

The eigenvalues of Hamiltonian (1) are found through diagonalization with the use of the Bogolyubov–Tyablikov transformation [14]. This leads to the following equation:

$$\det\|D^{\lambda\sigma}_{\alpha\beta}(\mathbf{k}) - \hbar\Omega(\mathbf{k})\delta_{\alpha\beta}\delta_{\lambda\sigma}\| = 0 \tag{3}$$

the solution of which gives the dispersion relation $\Omega(\mathbf{k})$, defining the elementary excitation spectrum.

Next, following the concepts developed in Refs. [9–11] regarding imperfect photonic structures and utilizing the virtual crystal approximation (VCA) [15,16], let us examine the dependence of the polaritonic excitation density of states in a topologically ordered defect—containing a two-sublattice chain of coupled microresonators with quantum dots—on the concentration of structural defects. For this purpose, it is convenient to express the configuration-dependent positions of micropores, whereby $a_{n1} = a^1_1\eta^1_{n1} + a^2_1\eta^2_{n1}$, $a_{n2} = a^1_2\eta^1_{n2} + a^2_2\eta^2_{n2}$, in terms of random variables. The positions of microcavities in the first and the second sublattices can be varied, thereby producing various types of crystals with different lattice constants, whereby $d_n = a_{n1} + a_{n2}$. Here, $\eta^{\nu}_{n1(2)}$ is a configuration-dependent random variable, and $\eta^{\nu}_{n1(2)} = 1$ if the position 1(2) of the resonator is de-

termined by the value $a^{\nu}_{1(2)}$ but is equal to 0 in any other case. As follows on from the configuration averaging technique [15,16], $\left\langle \eta^{\nu(\mu)}_{n1(2)} \right\rangle = \frac{N^{\nu(\mu)}_{1(2)}}{N} = C^{\nu(\mu)}_{1(2)}$, where $C^{\nu(\mu)}_{1(2)}$ is the concentration of resonators occupying a $\nu(\mu)$ position in 1(2) sublattices, and $N^{\nu(\mu)}_{1(2)}$ is the number of $\nu(\mu)$ grade positions in the first (second) sublattices.

Each of the tunnel-coupled resonators contains a single optical mode. Calculation of the quasiparticle excitation spectrum $\Omega(k)$ in a defect-containing photonic system is performed within the virtual crystal approximation with the use of an averaged Green's function apparatus [14,15]. Under these approximations, the averaged resolvent of the quasiparticle Hamiltonian is equal to the resolvent of the averaged Hamiltonian. This allows us to replace the quantities for $D^{\lambda\sigma}_{n\alpha,m\beta}$ in equality (1) by their configurationally averaged values, $D^{\lambda\sigma}_{n\alpha,m\beta} \to \left\langle D^{\lambda\sigma}_{n\alpha,m\beta} \right\rangle$. The procedure of configurationally averaging is carried out for all feasible positions of the resonators and is denoted by angular brackets. It "restores" the translation invariance and permits coming over to k-representation and the subsequent diagonalization of Hamiltonian through the Bogolyubov–Tyablikov transformation [14]. As a result, we arrive at Equation (3), which defines the dispersion spectrum of elementary excitations. The wave vector varies within the first Brillouin zone of the virtual lattice, with the period $\langle d_n \rangle = \langle a_{n1} \rangle + \langle a_{n2} \rangle = C^{(1)}_1 a^{(1)}_1 + C^{(2)}_1 a^{(2)}_1 + C^{(1)}_2 a^{(1)}_2 + C^{(2)}_2 a^{(2)}_2$. Obviously, $C^{(1)}_1 + C^{(2)}_1 = 1$ and $C^{(1)}_2 + C^{(2)}_2 = 1$; therefore, $C^{(2)}_1 = 1 - C^{(1)}_1 \equiv C_1$, $C^{(2)}_2 = 1 - C^{(1)}_2 \equiv C_2$. Hence, $\langle d \rangle = a_1(C_1) + a_2(C_2) \equiv d(C_1, C_2)$, where $a_1(C_1) = a^{(1)}_1 + \left(a^{(2)}_1 - a^{(1)}_1\right) C_1$ and $a_2(C_2) = a^{(1)}_2 + \left(a^{(2)}_2 - a^{(1)}_2\right) C_2$.

The quasiparticle spectrum shape must inevitably have an effect on the corresponding density of states, $\rho(\Omega)$. It has been our goal to use virtual crystal approximation to elucidate the dependence of the quasiparticle density of states $\rho(\Omega)$ on structural defect concentrations.

3. Results and Discussion

To address the above, general ideas, let us consider a defect-containing two-sublattice ($\alpha = 1,2; \beta = 1,2$) microresonator chain (see Figure 1), with same-type quantum dots embedded in one of the sublattices (e.g., in the first one). The concentrations of structural defects associated with variations in the microcavity positions are represented by C_1 and C_2.

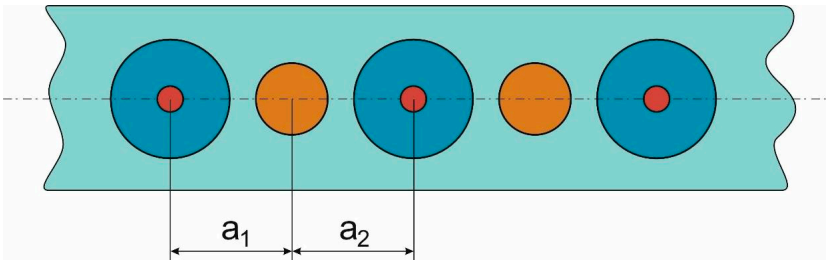

Figure 1. Schematic of a virtual two-sublattice chain of tunnel-coupled microcavities with embedded quantum dots. a_1, a_2 represent the positions of micropores in the first and second sublattices, obtained as a result of the configuration averaging of the structure under study.

The polaritonic spectrum $\Omega(\mathbf{k})$ of such a system is obtained according to the reasoning described in Ref. [13]. Diagonalization of the averaged Hamiltonian (1) and the use of approximations of the virtual crystals and nearest neighbors yield a system of homoge-

neous equations, the solvability condition of which is the equality to zero of the following determinant:

$$\begin{Vmatrix} \hbar\omega_1^{at} - V_{11}(k) - \hbar\Omega & g_1 & 0 \\ g_1 & \hbar\omega_1^{ph} - \hbar\Omega(k) & -A_{12}(k) \\ 0 & -A_{21}(k) & \hbar\omega_2^{ph} - \hbar\Omega(k) \end{Vmatrix} = 0 \quad (4)$$

Here, $A_{12(21)}$ is the Fourier transform of the matrix A_{n1m2}, which characterizes an overlap in the optical fields of resonators located at the **n**1 and **m**2 lattice nodes and, therefore, determines the probability of a tunnel transition of corresponding electromagnetic excitation; V_{11} is the Fourier transform of the matrix $V_{\mathbf{n1m1}}$ of the resonant interaction of quantum dots in nodes **n**1 and **m**1; g_1 is the parameter of the resonant interaction of a quantum dot in node **n**α, with an electromagnetic field localized in this node.

Finding the roots of the cubic equation with respect to frequency Ω, as yielded by the expansion of determinant (4), is performed with the use of the fzero.m standard library program in the MATLAB language for technical computing, based on Newton's iterative method. Since the QDs are all assumed to be of the same type, parameter g_1 of the resonance interaction between a QD and an electromagnetic field is the same at all sites.

Figure 2 shows 3D plots depicting the dependence of polaritonic dispersion $\Omega_{1,2,3}(k, C_1, C_2)$ in the considered system (the surfaces are numbered upward). Comparison of the shapes of the surfaces depicted in Figure 2a (obtained previously by the authors of Ref. [17]) and Figure 2b points to their smooth dependence on the value of parameter g; with an increase in the g value, the gap between the dispersion surfaces increases. The wave vector k varies within the first Brillouin zone: $-\frac{\pi}{d(C_1,C_2)} < k < \frac{\pi}{d(C_1,C_2)}$ (shaded region of the $\left(k, C_{1(2)}\right)$ plane in Figure 2).

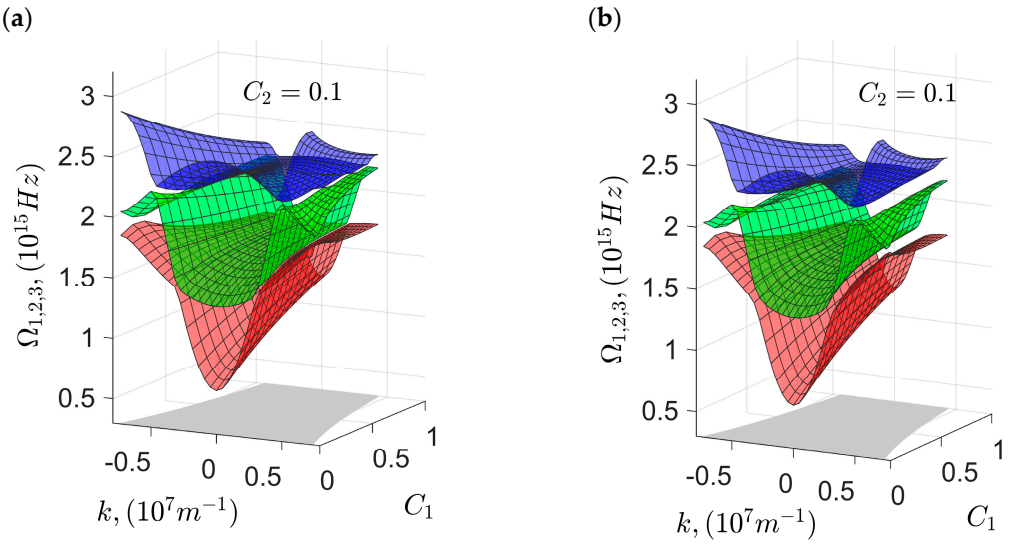

Figure 2. Polaritonic dispersion $\Omega_{1,2,3}$(k,C_1,C_2), plotted as a function of structural defect concentrations for a particular value of the parameter g $\equiv$ $g_1/\hbar$ of the resonance interaction between a QD and an electromagnetic field localized at the same site: (**a**) g = 10^{12} and (**b**) g = 10^{14}.

In this case, the expression for the density of states function $\rho_{1,2,3}(\Omega, C_1, C_2)$ takes the form of:

$$\rho_{1,2,3}(\Omega, C_1, C_2) = \frac{d(C_1, C_2)}{2\pi} \sum_i \frac{1}{\left|\frac{d\Omega_{1,2,3}(k, C_1, C_2)}{dk}\right|_{k_i}}. \quad (5)$$

We have performed a numerical evaluation of function (5) for wave vector k_i values falling in the first Brillouin zone for all three polaritonic branches.

In Figures 3–5, which depict functions $\rho_{1,2,3}(\Omega, C_1, C_2)$, one can clearly see the so-called Van Hove singularities, which arise due to the presence of local minima of functions $\Omega_{1,2,3}(k, C_1, C_2)$ in the k-space (see Figure 2). At these critical points (which may occur both at $k = 0$ and $k \neq 0$), the group velocity of the quasiparticle excitations changes to zero. The described peculiarities of the shape of spectrum $\Omega_3(k, C_1, C_2)$ in Figure 2, along with the singularities in Figure 5b,d, indicate the possibility of the formation of Bose–Einstein polaritonic condensate for certain concentrations of structural defects.

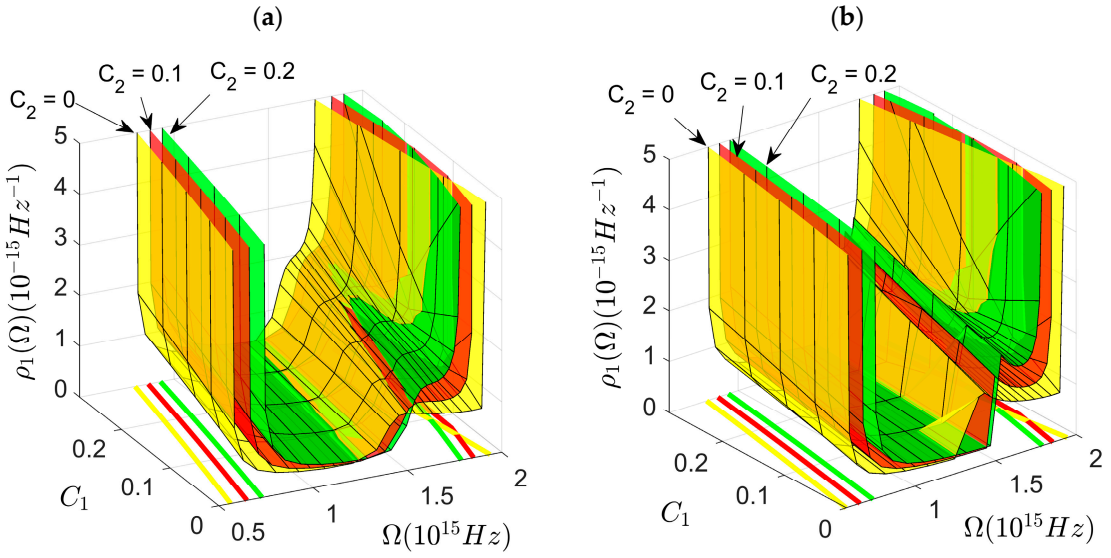

Figure 3. Density of the states in the first polaritonic branch (Figure 2), plotted for C_1 = 0; 0.1; 0.2, (**a**) g = 10^{14} Hz, (**b**) g = 10^{12} Hz.

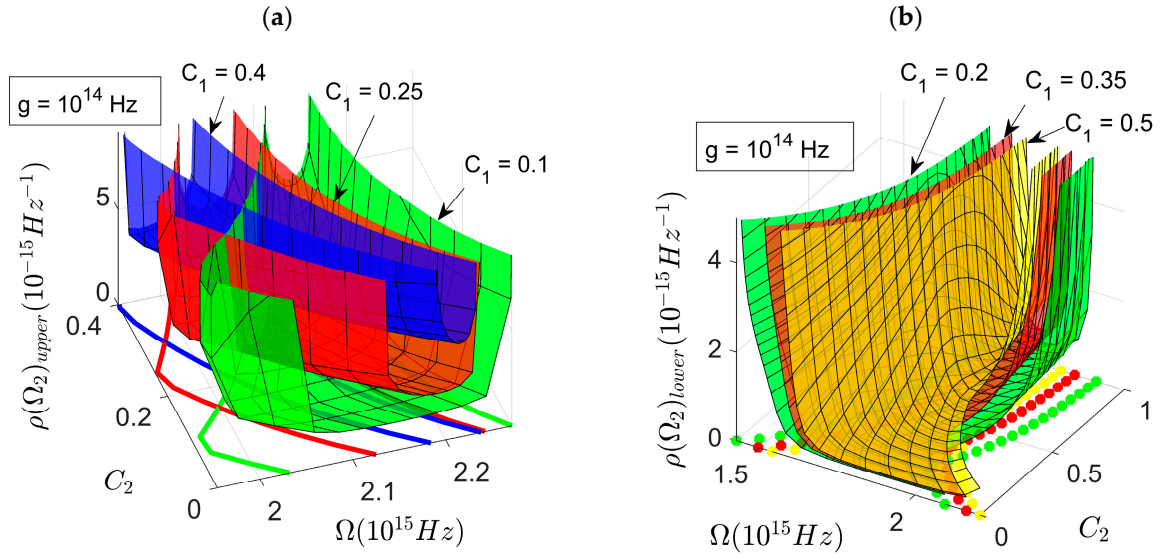

Figure 4. Densities of the polaritonic states plotted for: (**a**) the upper part of the second polaritonic branch (see Figure 2), where g = 10^{14} Hz, C_1 = 0.1; 0.25; 0.4, (**b**) the lower part of the second polaritonic branch, where g = 10^{14} Hz, C_1 = 0.2; 0.35; 0.5.

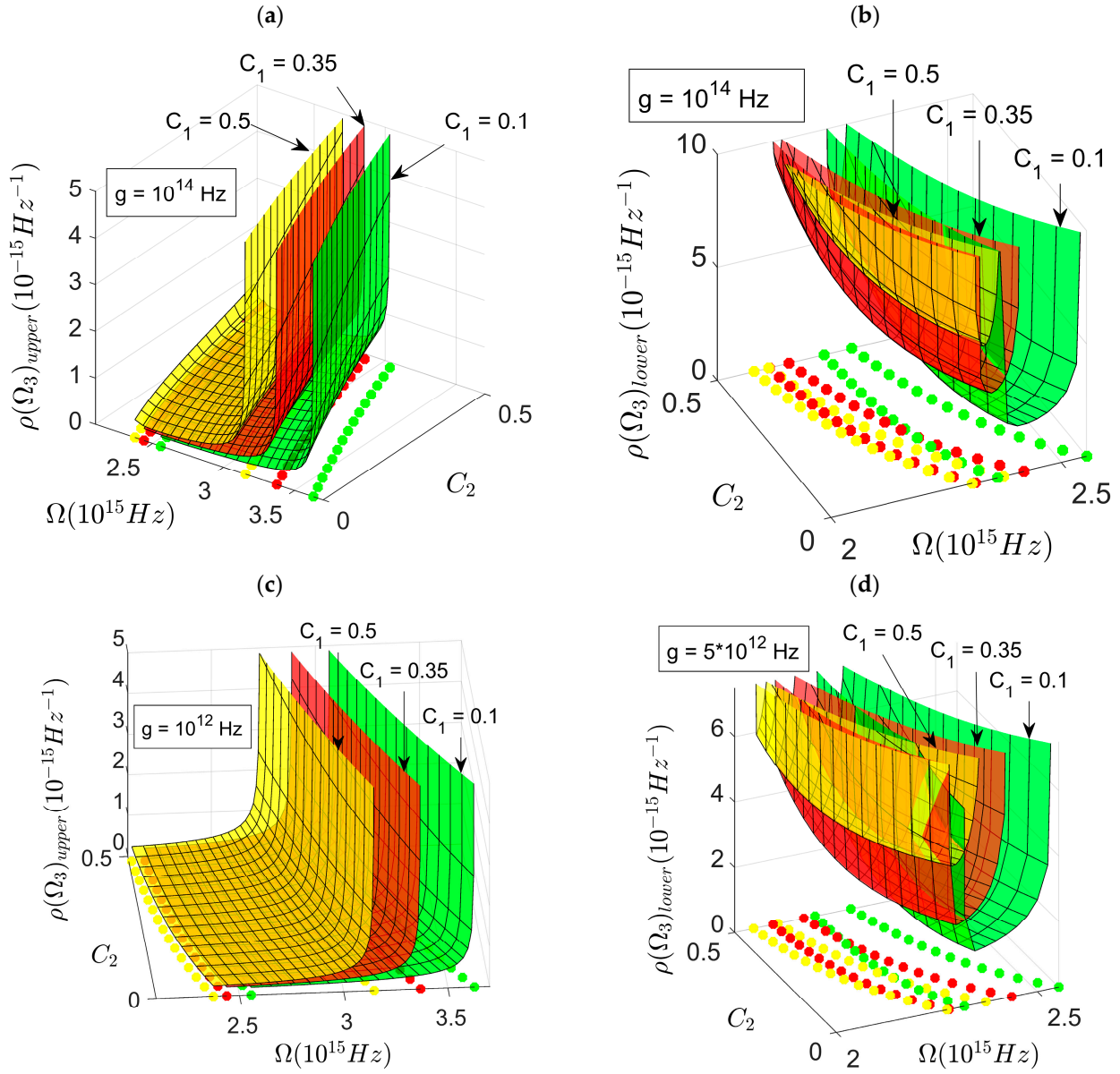

Figure 5. Densities of states in: (**a**) the upper part; (**b**) the lower part of the third polaritonic branch (Figure 2), for g = 10^{14} Hz, C_1 = 0.1; 0.35; 0.5; (**c**) the upper part of the second polaritonic branch for g = 10^{12} Hz, C_1 = 0.1; 0.35; 0.5; (**d**) the lower part of the second polaritonic branch (Figure 1) for g = 5×10^{12} Hz, C_1 = 0.1; 0.35; 0.5.

4. Conclusions

The obtained results reported in this study demonstrate the effect of changes in the spectrum of polaritonic excitations in a defect-containing one-dimensional microcavity lattice with embedded quantum dots on the corresponding density of states. We have employed virtual crystal approximation to calculate the dependence of the polaritonic density of states on the concentrations of structural defects associated with the variable positions of microcavities. It is also of interest to trace the renormalization of the energy structure of the crystal and the changes in its optical use, for example, in the framework of the approach [17,18], as well as to study the photon emission properties of a quantum dot cavity system via the master equation for the density matrix [19,20]. Our results also indicate the possibility of the formation of Bose–Einstein polaritonic condensate due to the presence of local minima in the quasiparticle spectrum $\Omega(\mathbf{k})$, both for $k = 0$ and (which is a less common phenomenon).

Author Contributions: Conceptualization, V.V.R.; formal analysis, V.V.R. and S.A.F.; investigation, V.V.R., S.A.F., K.V.G. and A.Y.R.; resources, V.V.R.; data curation, S.A.F. and A.Y.R.; writing—original draft preparation, V.V.R. and K.V.G.; writing—review and editing, V.V.R.; visualization, K.V.G.; supervision, V.V.R.; project administration, V.V.R.; funding acquisition, V.V.R. All authors have read and agreed to the published version of the manuscript.

Funding: This research received no external funding.

Data Availability Statement: Mathematical modeling has been performed with the use of the fzero.m standard library program in the MATLAB language of technical computing, based on Newton's iterative method. The model information of the group of Prof. P. Lodahl from Niels Bohr Institute, the University of Copenhagen, and the numerical data of Prof. A.P. Alojants at ITMO University (Russia) was used in the work.

Acknowledgments: The authors thank Kavokin A.V. for participating in the discussion of the model proposed in the work, which is reflected in joint publications.

Conflicts of Interest: The authors declare no conflict of interest.

References

1. Söllner, I.; Mahmoodian, S.; Hansen, S.L.; Midolo, L.; Javadi, A.; Kiršanskė, G.; Pregnolato, T.; El-Ella, H.; Lee, E.H.; Song, J.D.; et al. Deterministic photon–emitter coupling in chiral photonic circuits. *Nat. Nanotechnol.* **2015**, *10*, 775. [CrossRef] [PubMed]
2. Lodahl, P. Quantum-dot based photonic quantum networks. *Quantum Sci. Technol.* **2018**, *3*, 013001. [CrossRef]
3. Sedov, E.S.; Alodjants, A.P.; Arakelian, S.M.; Chuang, Y.-L.; Lin, Y.Y.; Yang, W.-X.; Lee, R.-K. Tunneling-assisted optical information storage with lattice polariton solitons in cavity-QED arrays. *Phys. Rev. A* **2014**, *89*, 033828. [CrossRef]
4. Joannopoulos, J.D.; Johnso, S.G.; Winn, J.N.; Meade, R.D. Photonic Crystals. In *Molding the Flow of Light*, 2nd ed.; Princeton University Press: Princeton, NJ, USA, 2008.
5. Kaliteevskii, M.A. Coupled vertical microcavities. *Tech. Phys. Lett.* **1997**, *23*, 120–121. [CrossRef]
6. Vahala, K.J. Optical microcavities. *Nature* **2003**, *424*, 839–846. [CrossRef] [PubMed]
7. Tighineanu, P.; Sørensen, A.S.; Stobbe, S.; Lodahl, P. The Mesoscopic Nature of Quantum Dots in Photon Emission. In *Quantum Dots for Quantum Information Technologies*; Michler, P., Ed.; Nano-Optics and Nanophotonics; Springer: Cham, Switzerland, 2017.
8. Alodjants, A.P.; Barinov, I.O.; Arakelian, S.M. Strongly localized polaritons in an array of trapped two-level atoms interacting with a light field. *J. Phys. B At. Mol. Opt. Phys.* **2010**, *43*, 095502. [CrossRef]
9. Rumyantsev, V.V.; Fedorov, S.A.; Gumennyk, K.V.; Gurov, D.A.; Kavokin, A.V. Effects of elastic strain and structural defects on slow light modes in a one-dimensional array of microcavities. *Superlattices Microstruct.* **2018**, *120*, 642–649. [CrossRef]
10. Rumyantsev, V.V.; Fedorov, S.A.; Gumennyk, K.V.; Sychanova, M.V.; Kavokin, A.V. Exciton-like electromagnetic excitations in non-ideal microcavity supercrystals. *Nat. Sci. Rep.* **2014**, *4*, 6945. [CrossRef] [PubMed]
11. Rumyantsev, V.V.; Fedorov, S.A.; Gumennyk, K.V.; Sychanova, M.V.; Kavokin, A.V. Polaritons in a nonideal periodic array of microcavities. *Superlattices Microstruct.* **2016**, *89*, 409–418. [CrossRef]
12. Dmitriev, S.V.; Baimova, Y.A. Effect of elastic deformation on phonon spectrum and characteristics of gap discrete breathers in crystal with NaCl-type structure. *Tech. Phys. Lett.* **2011**, *37*, 451–454. [CrossRef]
13. Rumyantsev, V.V.; Fedorov, S.A.; Gumennyk, K.V.; Paladyan, Y.A. Electromagnetic excitations in a non-ideal two-sublattice microcavity chain. *Phys. B Condens. Matter.* **2019**, *571*, 296–300. [CrossRef]
14. Agranovich, V.M. *Theory of Excitons*; Nauka: Moscow, Russia, 1968.
15. Los', V.F. Projection operator method in the theory of disordered systems. I. Spectra of quasiparticles. *Theor. Math. Phys.* **1987**, *73*, 85–102. [CrossRef]
16. Ziman, J.M. *Models of Disorder: The Theoretical Physics of Homogeneously Disordered Systems*; Cambridge University Press: Cambridge, UK, 1979.
17. Rumyantsev, V.V.; Fedorov, S.A. Novel Materials Based on Nonideal Supercrystal Formed by a Tunnel Connected Array of Microcavities Containing Ensembles of Quantum Dots. *J. Mater. Polym. Sci.* **2022**, *2*, 1–8.
18. Rumyantsev, V.V.; Fedorov, S.A.; Gumennyk, K.V.; Rybalka, A.; Zavorotnev, Y.D. Polaritonic crystal formed of a tunnel-coupled microcavity array and an ensemble of quantum dots. *J. Phys. Conf. Series* **2021**, *2052*, 012036. [CrossRef]
19. Yao, P.; Pathak, P.K.; Illes, E.; Hughes, S.; Münch, S.; Reitzenstein, S.; Franeck, P.; Löffler, A.; Heindel, T.; Höfling, S.; et al. Nonlinear photoluminescence spectra from a quantum-dot–cavity system: Interplay of pump-induced stimulated emission and anharmonic cavity QED. *Phys. Rev. B* **2010**, *81*, 033309. [CrossRef]
20. Diguna, L.J.; Darma, Y.; Birowosuto, M.D. The coupling of single-photon exciton–biexciton quantum dot and cavity. *J. Nonlinear Opt. Phys. Mater.* **2017**, *26*, 1750029. [CrossRef]